environmental microbiology

Environmental Microbiology (2016) **18**(1), 146–158 doi:10.1111/1462-2920.12924

Organic matter quantity and source affects microbial community structure and function following volcanic eruption on Kasatochi Island, Alaska

Lydia H. Zeglin,[1*†] Bronwen Wang,[1] Christopher Waythomas,[2] Frederick Rainey[3] and Sandra L. Talbot[1]

[1]*Alaska Science Center and*

[2]*Alaska Volcano Observatory, U. S. Geological Survey, Anchorage, AK, USA.*

[3]*Department of Biological Sciences, University of Alaska Anchorage, Anchorage, AK, USA.*

Summary

In August 2008, Kasatochi volcano erupted and buried a small island in pyroclastic deposits and fine ash; since then, microbes, plants and birds have begun to re-colonize the initially sterile surface. Five years post-eruption, bacterial 16S rRNA gene and fungal internal transcribed spacer (ITS) copy numbers and extracellular enzyme activity (EEA) potentials were one to two orders of magnitude greater in pyroclastic materials with organic matter (OM) inputs relative to those without, despite minimal accumulation of OM (< 0.2%C). When normalized by OM levels, post-eruptive surfaces with OM inputs had the highest β-glucosidase, phosphatase, NAGase and cellobiohydrolase activities, and had microbial population sizes approaching those in reference soils. In contrast, the strongest factor determining bacterial community composition was the dominance of plants versus birds as OM input vectors. Although soil pH ranged from 3.9 to 7.0, and %C ranged 100×, differentiation between plant- and bird-associated microbial communities suggested that cell dispersal or nutrient availability are more likely drivers of assembly than pH or OM content. This study exemplifies the complex relationship between microbial cell dispersal, soil geochemistry, and microbial structure and function; and illustrates the potential for soil microbiota to be resilient to disturbance.

Received 11 March, 2015; accepted 26 May, 2015. *For correspondence. E-mail lzeglin@ksu.edu; Tel. 785-532-5579; Fax 785-532-6653. †Present address: Division of Biology, Kansas State University, 116 Ackert Hall, Manhattan, KS 66506, USA.

Introduction

After a major volcanic eruption, recovery of above- and belowground components of the terrestrial ecosystem are linked (Halvorson *et al.*, 2005; DeGange *et al.*, 2010). New inputs of organic matter (OM) to fresh volcanic surfaces and disturbed soils may occur as plant or microbial autotrophic activity, both of which deposit metabolites and detritus to the developing soil; or OM may be imported from some outside source. In turn, soil microbial communities drive OM decomposition and mineral-weathering processes that make nutrients available to support further plant and microbial production and the development of above- and belowground food webs (Schlesinger, 1997; Whitman *et al.*, 1998; Fenchel *et al.*, 2000). The availability of carbon and nutrients in developing soils constrains ecosystem recovery from disturbance (Vitousek and Farrington, 1997), and may help determine the succession of terrestrial biota (Odum, 1969). Microbial activity in new volcanic deposits is therefore a key component of soil and ecosystem recovery post-eruption, yet the factors determining establishment of a functional soil microbial community following eruption are rarely studied.

The trajectory of soil microbial community establishment following a major volcanic eruption depends on the colonization of new cells and the availability of energy to fuel cell growth (Fierer *et al.*, 2010). Vectors of cell dispersal for colonization may include long-distance atmospheric deposition, local aeolian redistribution of sediment (Sabacka *et al.*, 2012; Smith *et al.*, 2013) or colonizing plants and animals that carry microbiota on their tissues or in their guts. Energy and nutrients may be provided by animal-borne inputs of OM (Croll *et al.*, 2005; Leblans *et al.*, 2014), or newly fixed carbon (C) from plant photosynthesis (Halvorson *et al.*, 1992; Ibekwe *et al.*, 2007; Halvorson and Smith, 2009). In the absence of OM input from external sources to drive microbial heterotrophy, microbial photo- or chemolithoautotrophy must fuel cell growth (King, 2003; Nemergut *et al.*, 2007). Thus, the contrasting sources of OM and microbial cells to soils recovering from volcanic disturbance may create alternative states in the recovery of microbial community structure and function (Odum, 1969; Fierer *et al.*, 2010).

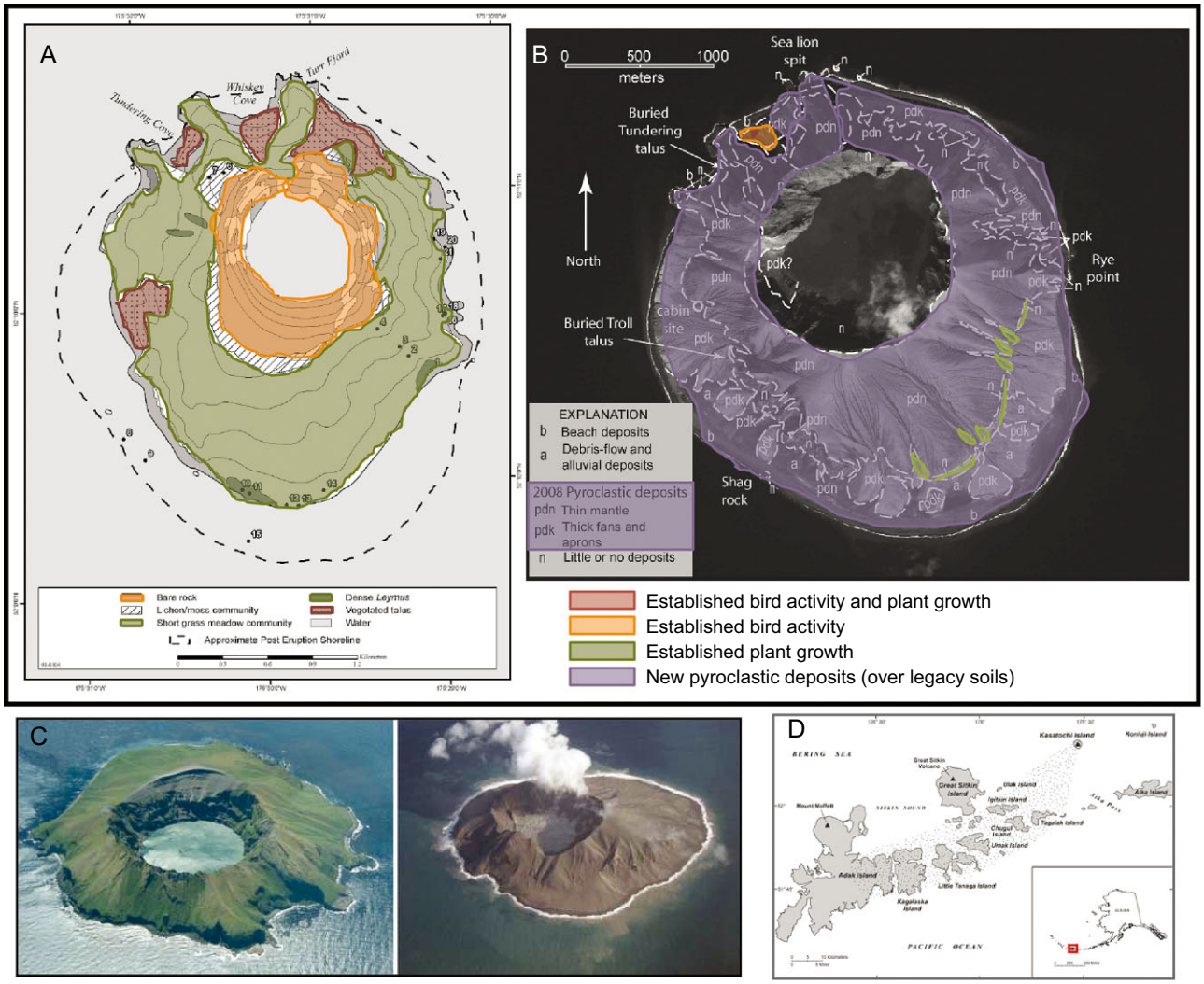

Fig. 1. Map of (A) pre- and (B) post-eruptive Kasatochi Island, with areal coverage of bird activity and plant inputs (red), bird activity (orange), established plant growth (green) and 2008 pyroclastic deposits (purple) overlaid (maps modified from Scott *et al.*, 2010; Talbot *et al.*, 2010); (C) aerial photos of Kasatochi Island pre- and post-eruption; (D) regional map of the study area, with zoom area highlighted in red in the inset.

The influence of OM input and cell dispersal on soil microbial community development can be evaluated on Kasatochi Island, a small volcanic island located in the west central Aleutian Islands, Alaska, USA (Fig. 1). The Aleutian Islands experience high levels of volcanic activity, driven by subduction along the Aleutian Trench (Miller *et al.*, 1998; Jicha *et al.*, 2006). A recent, dramatic example of this activity occurred in August 2008, when the eruption of Kasatochi volcano covered Kasatochi Island with pyroclastic material and ash up to 10s of metres thick (Scott *et al.*, 2010). This event buried the entire island and destroyed seabird rookeries and lush meadows (DeGange *et al.*, 2010), which are biologically rich and productive communities typical of the Aleutian Islands. Rapid erosion of the volcanic deposits has exposed pre-eruptive soils on high ridges and within gullies (Waythomas *et al.*, 2010), and plant regrowth is evident in most places where these 'legacy' soils are at or near the current surface (Talbot *et al.*, 2010; Walker *et al.*, 2013). Nesting seabirds have also returned to post-eruptive surfaces (Williams *et al.*, 2010). As plant and bird communities develop on these new surfaces, creating a mosaic of contrasting cell and OM inputs, it is critical to study the concurrent recovery of soil microbial communities.

To assess the level of re-establishment of soil microbiota on Kasatochi Island 5 years post-eruption, samples of the 2008 pyroclastic deposits and pre-eruptive legacy soils with contrasting OM inputs were collected in 2013, and their geochemistry, microbial function and diversity were measured. We hypothesized that the recovery of soil microbial structure and function would be related primarily to energy availability (Odum, 1969; Fierer *et al.*, 2010). Specifically, we expected that microbial activities and population sizes would be correlated with

total OM accumulation, assuming OM is the main energy source promoting microbial recovery. Also, we expected that surface samples of volcanic deposits with and without OM inputs would contain distinct microbial communities. The data show clear impacts of both OM amount and source on soil microbial re-establishment, with trajectories of community assembly decoupled from recovery of functional activity.

Results

Soil geochemical characteristics

Pyroclastic deposits from the 2008 eruption and legacy soil samples from Kasatochi Island spanned a wide range in C and N contents (0.05–16.7% C and < 0.01–1.4% N) and a moderate range in other geochemical variables (Table S1). Legacy soils had higher water content, cation exchange capacity (CEC), %C and %N, extractable NH_4^+-N, NO_3^--N and P, molar C : P and N : P, and lower pH, than the recent pyroclastic deposits. Samples with post-eruption bird inputs had higher %C, extractable NH_4^+-N, NO_3^--N and P and lower pH than samples without post-eruption bird inputs. Samples with post-eruption plant growth inputs had higher extractable P and lower pH, CEC and base saturation (BS) than samples without post-eruption plant growth inputs. There were interactive legacy-by-plant effects on pH, CEC, %C and %N and extractable P levels, and bird-by-plant effects on extractable NH_4^+-N and NO_3^--N levels. Neither molar C : N ratio nor electrical conductivity (EC) varied significantly among any groups of samples ($P > 0.05$).

Soil extracellular enzyme activity (EEA) potential

Potential EEA for hydrolytic enzymes ranged from the 10s to 10 000s of nmol methylumbelliferyl (MUB) or amino-methylcoumarin (AMC) g^{-1} OM h^{-1}, and for oxidative enzymes ranged from 1s to 1000s of μmol L-3,4-dihydroxyphenylalanine (L-DOPA) g^{-1} OM h^{-1} (Table S2). Decay of substrate was below detection level for a number of samples in phosphatase (Phos), leucyl aminopeptidase (LAP), cellobiohydrolase (CBH) and oxidative enzyme assays, so these rates were recorded as zero; positive substrate decay was detected for all samples in β-glucosidase (βG) and *N*-acetylglucosaminidase (NAG) enzyme assays. Legacy soils had higher OM-specific LAP potential activity, and lower OM-specific POX potential activities than pyroclastics; βG, Phos and NAG activities were higher in legacy soils than bare pyroclastics, but lower in legacy soils than pyroclastics with OM inputs; CBH activities were higher in legacy soils than bare pyroclastics, but lower in legacy soils than pyroclastics with plant OM inputs (Fig. 4, Fig. S1, Table S2). Samples with post-eruption bird inputs had higher βG, Phos and NAG potential activity, and lower peroxidase (POX) potential activity than samples without post-eruption bird inputs. Samples with post-eruption plant growth inputs had higher βG, Phos, NAG and CBH potential activity than samples without post-eruption plant growth inputs. There were interactive legacy-by-plant effects on βG, Phos and CBH potential activities, and interactive bird-by-plant effects on βG and NAG activities. Phenol oxidase (PHX) potential activity did not vary significantly among any groups of samples ($P > 0.05$).

Principal components analysis (PCA) reduced the seven EEA variables to two axes (PC1 and PC2) that described 63.0% of the variability in the EEA data. Activities of all enzymes except LAP influenced these two axes, with hydrolytic activities loading in the negative direction on the first axis and oxidative activities loading in the positive direction on the second axis (Table 1, Fig. 2A). There were primary and interactive effects of all OM input groups on distribution of samples along PC1, and legacy soils were distributed significantly lower on PC2 than pyroclastic samples (Table S2). Soil chemical and microbial variables that significantly correlated with PC axes included pH, fungal ITS and bacterial 16S rRNA gene

Table 1. Extracellular enzyme loadings on PC axes, and significant correlations between NMDS axes and abundance or relative abundance of microbial groups.

EEA loadings	PC1 (47.5%)	PC2 (15.5%)
β-glucosidase	**–0.521**	0.115
Phosphatase	**–0.439**	–0.133
N-acetylglucosamine	**–0.488**	0.164
Cellobiohydrolase	**–0.474**	0.101
L-aminopeptidase	–0.182	0.028
Phenol oxidase	0.035	**0.796**
Peroxidase	0.197	**0.545**
Microbial population sizes	**NMDS 1 R, p**	**NMDS 2 R, p**
Acidobacteria	**0.810, < 0.0001**	–0.105, 0.44
Nitrospirae	**0.707, < 0.0001**	–0.110, 0.42
Verrucomicrobia	**0.696, < 0.0001**	–0.115, 0.40
Deltaproteobacteria	**0.660, < 0.0001**	–0.044, 0.75
Bacteria, Other	**0.659, < 0.0001**	0.129, 0.34
Planctomycetes	**0.614, < 0.0001**	–0.298, 0.03
Chloroflexi	**0.580, < 0.0001**	–0.283, 0.04
Fungal ITS copy #	0.306, 0.01	**–0.659, < 0.0001**
Bacterial 16S rRNA gene copy #	0.254, 0.01	**–0.663, < 0.0001**
Alphaproteobacteria	0.127, 0.35	**–0.506, < 0.0001**
Aquificae	–0.107, 0.43	**0.628, < 0.0001**
Gammaproteobacteria	**–0.447, 0.0005**	0.418, 0.001
Cyanobacteria	**–0.477, 0.0002**	–0.031, 0.82
Betaproteobacteria	**–0.606, < 0.0001**	0.270, 0.05
Bacteroidetes	**–0.697, < 0.0001**	–0.195, 0.15

Values in **bold** highlight PCA eigenvalues > |0.4|, or significant ($P \leq 0.001$) correlations with microbial group abundance (non-significant variables are not listed). R is the Pearson's R correlation coefficient.

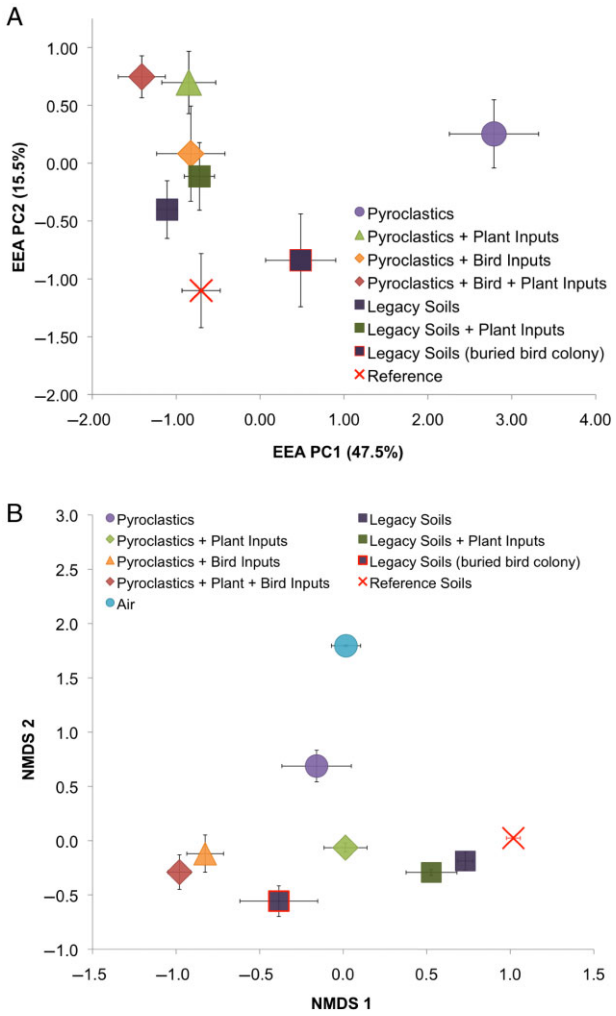

Fig. 2. (A) Principal components analysis ordination of seven classes of extracellular enzyme activity potential for each OM input category (mean ± 1SE). Individual enzyme activity loadings are shown in Table 1. (B) Non-metric multidimensional scaling ordination of the relative abundance of 97% similar bacterial 16S rRNA gene taxonomic units for each OM input category (mean ± 1SE). Correlations of axes with major taxonomic group abundances are shown in Table 1, and different symbols are used for contrasting OM input categories, including highlighted differentiation of legacy soils from the buried bird colony.

copy numbers, fungal ITS: bacterial 16S rRNA gene copy ratio, water content, DNA yield, %C and %N, C : N ratio, and extractable inorganic N and P concentrations (Fig. S2A, Table S3).

Bacterial and fungal population size and diversity

Bacterial 16S rRNA genes and fungal ITS copies were detectable in all samples: based on standard curves, a threshold of 114 bacterial 16S rRNA gene copies per reaction or 25 fungal ITS copies per reaction could be quantified. After accounting for DNA yield, bacterial 16S rRNA gene copies ranged from 2.3×10^4 to 1.8×10^{10} g^{-1} of dry soil, and fungal ITS copies ranged from 5.0×10^3 to 3.9×10^8 g^{-1} of dry soil; also, DNA yield ranged from 0.2 to 25 μg DNA g^{-1} of dry soil, and the ratio of fungal : bacterial (F : B) gene copies ranged from 0.004 to 0.64 (Fig. 4, Table S4). Legacy soils had higher DNA yields, 16S rRNA gene copies and ITS copies than pyroclastic samples. Samples with post-eruption bird inputs had higher DNA yields, 16S rRNA gene copies and ITS copies than samples without post-eruption bird inputs. Samples with post-eruption plant growth inputs had higher 16S rRNA gene copies, ITS copies and F : B than samples without post-eruption plant growth inputs. There were interactive legacy-by-plant effects on DNA yields, 16S rRNA gene copies, ITS copies and F : B, and interactive bird-by-plant effects on 16S rRNA gene copies and F : B.

The number of unique 97% similar bacterial 16S rRNA gene sequence operational taxonomic units (OTUs) per sample ranged from 1077 to 7849, the Chao1 estimated richness ranged from 1453 to 10 135, Shannon's diversity ranged from 5.42 to 10.46, equitability ranged from 0.498 to 0.871 and samplewise Bray–Curtis dissimilarity ranged from 0.759 to 0.964. Legacy soils had greater OTU numbers and Chao1 richness than pyroclastic samples (Table S4). Samples with post-eruption bird inputs had lower Chao1 richness, diversity and evenness, and greater dissimilarity, than samples without post-eruption bird inputs. Samples with post-eruption plant growth inputs had greater OTU numbers, Chao1 richness and diversity, and lower dissimilarity, than samples without post-eruption plant growth inputs. There were interactive bird-by-plant effects on OTU numbers and Chao1 richness.

Bacterial community composition

The non-metric multidimensional scaling (NMDS) ordination of bacterial 16S rRNA OTU relative abundances produced a consistent three-dimensional model solution with stress = 0.0918 (Fig. 2B) and the permutational multivariate analysis of variance (PERMANOVA) results showed significant ($P < 0.05$) legacy, plant and bird effects, and interactive plant by bird effects, on bacterial community composition. Sample positions along the first NMDS axis were significantly differentiated among legacy and bird-input groups, with no interactive effects, and sample positions along the second NMDS axis were significantly differentiated by legacy, plant and bird-input groups, with legacy-by-plant and bird-by-plant interactive effects (Table S4). NMDS axes were correlated with the relative abundance of many dominant bacterial phyla and subphyla (Table 1), and many soil chemical and microbial properties (Fig. S2B, Table S3).

The relative abundance of all phyla except *Acidobacteria* and *Bacteroidetes* differed significantly

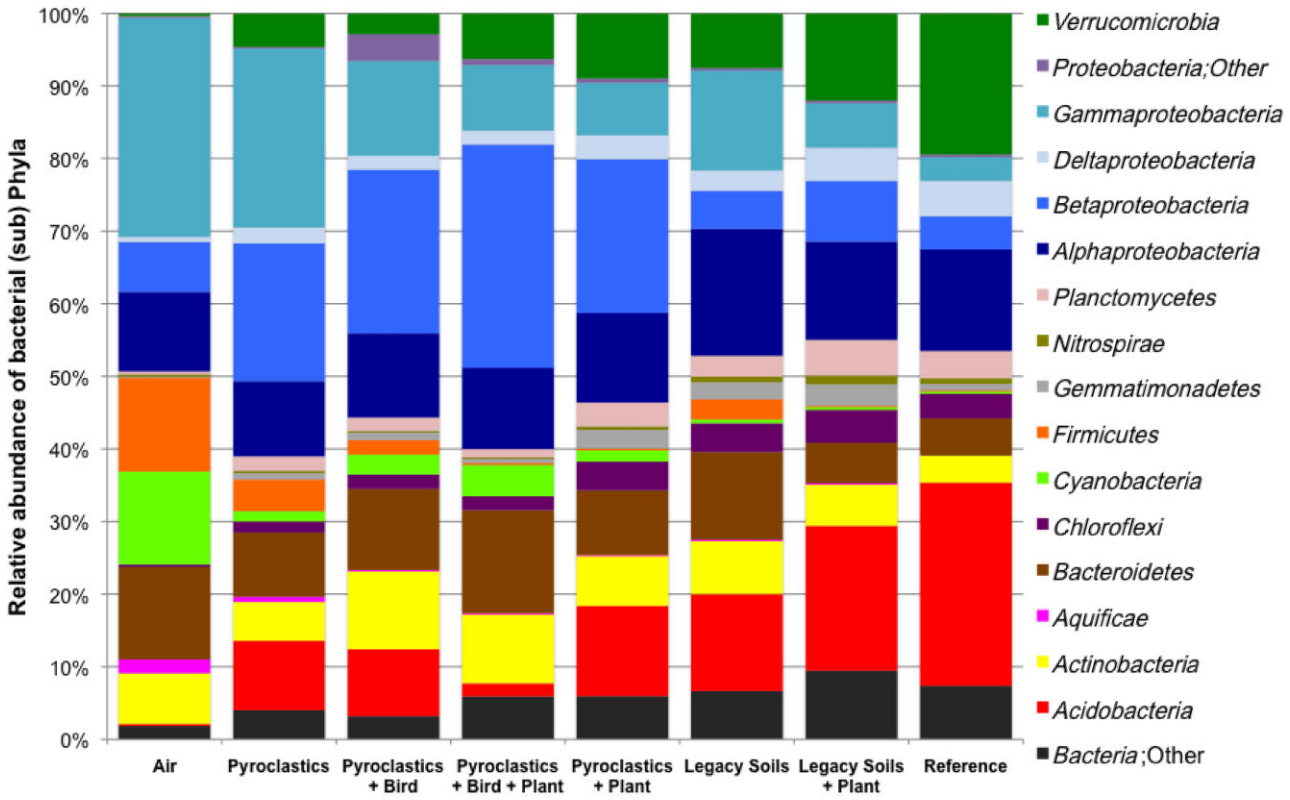

Fig. 3. Relative abundance of 97% similar bacterial 16S rRNA gene taxonomic units in abundant bacterial phyla (and Proteobacterial subphyla) for each OM input category.

($P < 0.05$) between pyroclastic deposits and legacy soils, or between samples with and without bird or plant inputs (Fig. 3, Table S5). Most notably among these differences, pyroclastic deposit samples had higher relative abundance of *Aquificae* and *Betaproteobacteria*, and lower relative abundance of *Alphaproteobacteria* and *Verrucomicrobia* than legacy soil samples; samples with post-eruption plant growth inputs had lower relative abundance of *Aquificae*, *Firmicutes*, *Gammaproteobacteria* and higher relative abundance of *Verrucomicrobia* than samples without post-eruption plant growth inputs; and samples with post-eruption bird inputs had higher relative abundance of *Actinobacteria*, *Aquificae* and *Cyanobacteria* than samples without post-eruption inputs.

The Venn diagram of all samples showed that the greatest number of unique OTUs was found in legacy soils, followed by air samples and bare pyroclastics and that reference soils had the fewest number of unique OTUs, that core OTU overlap with bare pyroclastics was seven times greater in legacy soils than air samples, and that less than 1% of core OTUs were found in all four groups (Fig. S3A). The Venn diagram of pyroclastic samples only showed that the greatest number of unique OTUs was found in pyroclastic materials with plant inputs, that core OTU overlap with bare pyroclastic deposits was more than two times greater where plant inputs were present in comparison to where bird inputs were present and that 5% of core OTUs were found in all pyroclastic samples (Fig. S3B).

Discussion

Five years following the August 2008 Kasatochi eruption, diverse and functional microbial communities had developed in the initially sterile pyroclastic deposits. Recovery status was linked to soil geochemical conditions and to sources of colonizing microbial cells. These results underscore the high potential for resilience of microbial life following extreme disturbance, contingent upon the return of habitat conditions favourable to metabolic activity. Also, the composition of the developing microbial communities was more closely related to the presence of birds versus plants than to soil pH or carbon content: this has strong implications for the relative importance of geochemical constraints versus cell dispersal in the succession of soil microbial diversity and function.

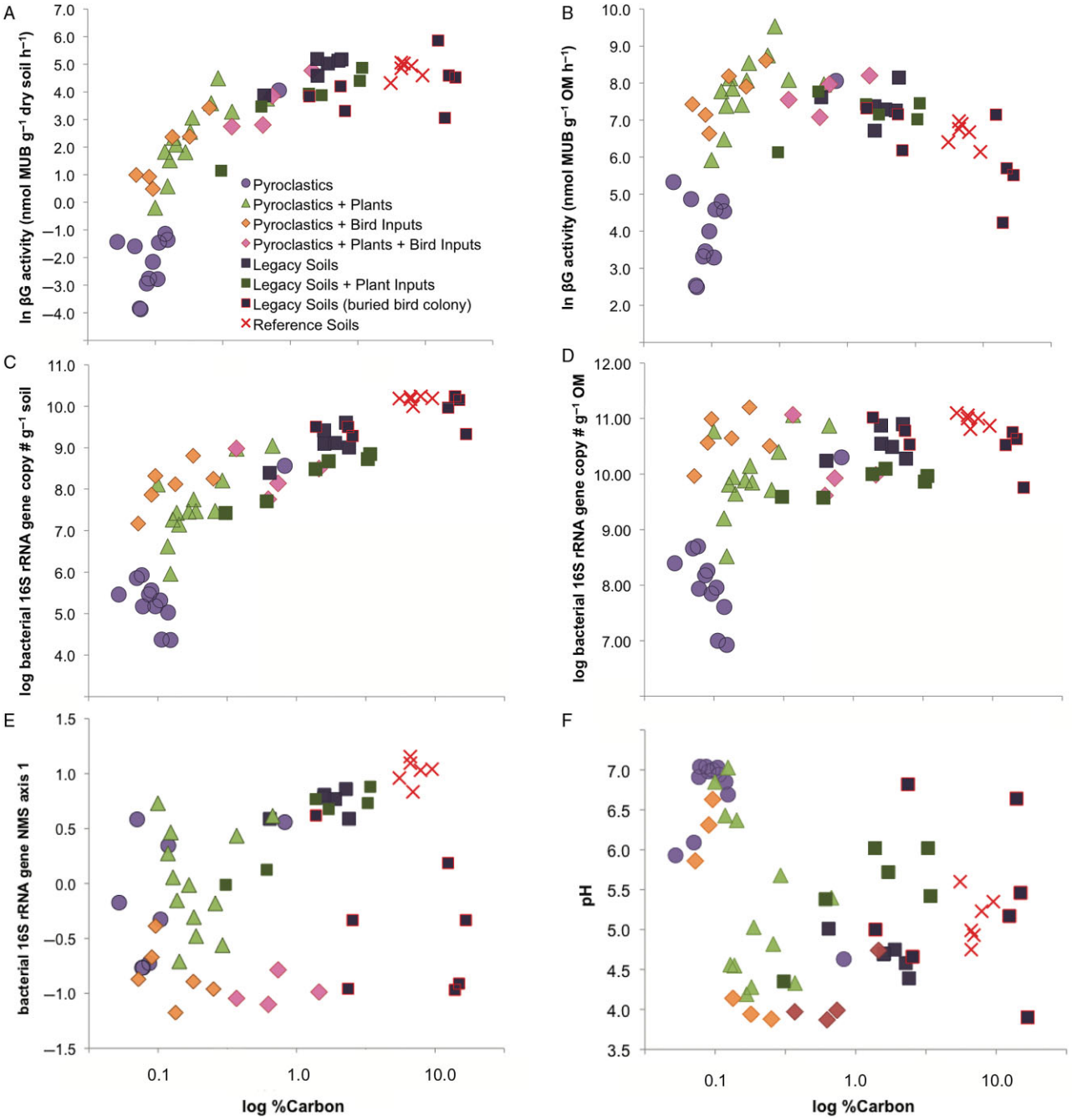

Fig. 4. Scatterplots of soil % carbon versus soil microbial βG activity potential (A) per gram of dry soil and (B) per gram of OM; versus soil bacterial 16S rRNA gene copy number (C) per gram of dry soil and (D) per gram of OM; versus (E) bacterial 16S rRNA gene community NMS ordination axis 1; and versus (F) soil ph, with different symbols for contrasting OM input categories including highlighted differentiation of legacy soils from the buried bird colony.

Microbial growth and activity post-volcanic eruption

The quantitative measurements of microbial molecular signatures show evidence for bacterial and fungal biomass growth and production of extracellular enzymes in the recent pyroclastic deposits, particularly in the presence of OM inputs. Pyroclastic materials with plant and bird OM inputs support two to three orders of magnitude greater bacterial and fungal gene copy numbers g^{-1} of soil, and up to one to two orders of magnitude greater hydrolytic EEA rates g^{-1} OM h^{-1}, relative to adjacent pyroclastics without birds or plants (Table S2, S4, Fig. 4, Fig. S1). The higher levels of microbial ribosomal genes and enzymes on these surfaces are evidence of

post-eruptive *in situ* growth stimulated by OM inputs. In contrast, molecules detected on bare pyroclastic deposits may have been produced by microbiota active *in situ*, or may be present due to atmospheric deposition or aeolian redistribution of cells from adjacent surfaces. Although microbial respiration or productivity was not measured directly in this study, CO_2 efflux from bare pyroclastic materials was detected in 2011 (Michaelson *et al*., 2014), only 2 years after the eruption, indicative of *in situ* metabolic activity. These observations all support the conclusion that OM inputs, although small in magnitude, have supported significant levels of microbial growth and activity on initially sterile pyroclastic deposits in the 5 years since eruption.

Microbial population sizes and activities in the recent pyroclastic deposits are lower on a dry mass basis, but similar on an OM basis, to levels found in pre-eruptive legacy soil, regional reference soil and 'typical' soils globally (Sinsabaugh *et al*., 2008; Yarwood *et al*., 2010). Microbial populations in legacy soils suggest the possibility of survival of a subset of the pre-eruptive community and/or greater microbial growth after the 2008 eruption, supported by significant levels of remnant OM. Legacy soil recovery to pre-eruption conditions may be incomplete because microbial population estimates in Kasatochi legacy soils averaged one to two orders of magnitude lower per gram of soil than regional reference soils, and average soil %C was 0.8–2.5 times lower (Fig. 4, Table S4). Likewise, microbial population estimates in pyroclastic materials with OM inputs averaged two to three orders of magnitude lower per gram than regional reference soils, and %C was one to two orders of magnitude lower. As a function of soil OM, however, microbial populations in pyroclastic deposits with OM inputs are booming, reaching copy numbers comparable with legacy and reference soils containing 10 times more C (Fig. 4, Table S4). Similarly, enzyme activities were as high or higher in both legacy soils and pyroclastic deposits with OM inputs than in regional reference soils, on an OM-specific basis (Fig. 4, Table S2). Overall, βG activity levels in bare pyroclastics are in the same very low range as Antarctic Dry Valleys soils [where there is no plant-derived OM (Zeglin *et al*., 2009)], whereas pyroclastic deposits with trace OM inputs have OM-specific microbial enzyme and population densities approaching levels characteristic of fully developed soils (Sinsabaugh *et al*., 2008; Yarwood *et al*., 2010), 5 years post-eruption.

Interactions between nutrient availability, OM quality and microbial community composition might underlie the concurrent development of structure and function, and the complex data set hints at these mechanisms. Both available N and Phos potential activity were highest in bird-impacted pyroclastic materials (Table S1, Fig. S2B), indicating a microbial community likely to be developing under relatively P-limited conditions. In contrast, cellulolytic potential activity, EEA PC2 (oxidative enzyme potential activity) and F : B ratio were all higher in samples with new plant OM inputs (Tables S1, S4, Fig. S2A), suggesting that fungal population growth might be more closely linked to decomposition of fresh plant litter. Extracellular enzymes can be produced by both fungi and bacteria, but not all microbial taxa sacrifice energy that could be used for growth to support enzyme expression (Allison, 2005). It is possible that these more slowly growing microbial taxa thrive in habitats with lower OM availability (Fierer *et al*., 2007), whereas taxa with higher growth rates are more associated with labile, complex OM availability (Klappenbach *et al*., 2000). If r- versus K-growth strategies are in fact reflected by 16S rRNA gene copy number, this would help explain the high bacterial gene counts in low OM soils with fresh OM inputs. However, the distribution of phylum-relative abundance between legacy soils and pyroclastic surfaces does not necessarily fit predicted coherence of growth strategies at deeper taxonomic levels (Fierer *et al*., 2007; Philippot *et al*., 2010): e.g. although the putatively r-strategists *Betaproteobacteria* are least abundant in legacy soils, as expected, the putatively K-strategists *Verrucomicrobia* (Fierer *et al*., 2013) are most abundant in both legacy soils and samples with new plant OM input (Table 1, Fig. 3, Table S5). Some divergence from expected patterns in microbial structure and function may reflect the dynamic state of these early successional microbiota.

Geochemical constraints on microbial growth and activity post-eruption

Soil geochemical characteristics, particularly pH and %C, are broadly correlated with microbial structure and function (Sinsabaugh *et al*., 2008; Fierer *et al*., 2009; Lauber *et al*., 2009; Rousk *et al*., 2010). pH and %C reflect the integrated accumulation of acidity and OM respectively. Rapid abiotic weathering of bare surficial pyroclastic deposits on Kasatochi drove a pH drop from a mean of 8 at deposition (Wang *et al*., 2010) to a mean of 6.6 in 2013 (Table S1), and the 2013 pH was even lower in pyroclastics with OM inputs (mean 4.1–5.1, overlapping legacy soil and reference soil pH at means 5.1–5.6 and 5.1 respectively). In addition to abiotic weathering, bird, plant and microbial activity can produce acidity. Bird faeces contains uric acid (Bhattacharya and Fontenot, 1965), plant root exudates include organic acids (Griffiths *et al*., 1999) and plant roots and microorganisms respire, producing protons. Even with trace OM availability, heterotrophic bacterial growth on pyroclastic material can drive significant weathering, releasing soluble P and micronutrients (Wu *et al*., 2007; Cockell *et al*., 2009) and thus promoting further plant and microbial production.

There are correlations between pH and soil microbial community structure and function on post-eruption Kasatochi Island (Table S3); however, these relationships are driven by the considerable separation of bare pyroclastic deposits from all other samples (Fig. 2, Fig. S2), leaving no predictable relationship between pH and EEA, microbial population size or microbial community composition (Fig. 4). OM-poor pyroclastic surfaces may be particularly heterogeneous in pH due to low buffering capacity. Positive feedback between the accumulations of acidity, soil OM, microbial and plant biomass means that at this early stage in soil and ecosystem recovery from disturbance, pH and microbial community structure and function are changing concurrently; thus, pH is not an independent driver of microbial recovery on Kasatochi Island.

In contrast, %C is strongly correlated with EEA and microbial population sizes per gram of soil (Fig. 4). In volcanic soils, the accumulation of OM proceeds rapidly in the first decades following deposition of parent material (Zehetner, 2010). In this study, mean %C in the pyroclastic deposits with bird, plant, and bird and plant OM inputs was similar, 40% higher and 500% higher, respectively, than bare pyroclastic materials (Table S1). In addition to the positive feedback between biological weathering and C accumulation already discussed, positive feedback between bird-imported marine N and plant and microbial production is likely (Croll *et al*., 2005; Leblans *et al*., 2014), especially because plant production on Kasatochi Island is N-limited (Michaelson *et al*., 2014). There were also significantly higher bacterial populations in pyroclastics with bird inputs relative to pyroclastics with plant inputs and similar %C (Fig. 4, Table S4); in addition to N, bird droppings may carry a significant bacterial cell load. Overall however, no matter the OM source, the accumulation of soil C is clearly linked to the recovery of (presumably heterotrophic) microbial growth and activity.

Microbial community assembly post-eruption

Bacterial community composition was strongly differentiated among bare pyroclastics, pyroclastics with bird OM inputs and reference soils; pyroclastic deposits with plant OM inputs and legacy soils had more spatially heterogeneous assemblages, placing their average community state in an intermediate, yet distinct position relative to the other samples (Fig. 2B, Fig. S2B). Based on the uniqueness of the bird-impacted pyroclastic assemblages, we hypothesized that a key factor explaining legacy assemblage heterogeneity was the presence of pre-eruption bird OM inputs. In fact, legacy soils collected from the buried seabird colony contained bacterial communities more similar to recent pyroclastic deposits with bird inputs than to reference soils or legacy soils with no bird inputs, despite the overlap in pH, %C, microbial population sizes and enzyme activity levels with other legacy and reference soils (Fig. 4E). There may be distinct trajectories and endpoints to soil microbial community assembly post-eruption that are defined by the presence of plants or seabirds, yet independent of soil pH or OM accumulation.

The unique microbial communities characteristic of seabird colony surfaces could result from the input of specific taxa in bird guano, or from selection for taxa better adapted for survival in the soil conditions created by high seabird density. The bird guano bacterial load or community composition is currently unknown, but is certainly expected to contain a distinct microbiota. However, guano influx is not constant because seabirds roost only until chicks are fledged (June–July; birds were not present when samples were collected in mid-August), so distinct microbial populations must persist through periods with no supplemental cell or OM inputs, and through stochastic disturbances like volcanic eruption. The geochemical environment of bird-impacted surfaces differed significantly from plant-impacted surfaces only in having higher available N (Table S1). Higher nutrient availability could select for microbial taxa with different N kinetics, or an unmeasured ephemeral factor associated with bird presence could be strong enough to maintain this unique community composition. Either mechanism could explain the lower bacterial diversity and evenness in bird-impacted pyroclastic deposits (Table S4). Only 46 bacterial OTUs, from a breadth of phyla and subphyla, were found in all (both new and buried) bird colony samples (Text S1); the most commonly represented taxa included the genus *Salinibacterium* (Family *Microbacteriaceae*, *Actinobacteria*) and the family *Xanthomonadaceae* (*Gammaproteobacteria*),and the most abundant OTUs were two unidentified Betaproteobacterial and one *Xanthomonadaceae* taxon. It is not clear what these groups have in common, but the prevalence of one known halophilic genus (Kim and Nedashkovskaya, 2012) suggests that seabirds might be a vector for marine-derived cells. More work is necessary to understand the relative importance of environmental filtering and dispersal in shaping the trajectory of microbial community assembly in these developing soils (Logue *et al*., 2011).

Bacterial communities on bare pyroclastic surfaces were indeed distinct from other sample types; however, it is not clear whether autotrophic metabolic strategies dominated this earliest successional assemblage, as might be expected (Nemergut *et al*., 2007): photoautotrophic Cyanobacterial taxa actually had higher relative abundance in bird-impacted than bare pyroclastic deposits (Table S5). However, prevalence of chemolithoautotrophy is difficult to establish with 16S rRNA gene data because chemolithoautotrophy is diverse, paraphyletic and often facultative. Bacterial phyla found in bare pyroclastic

materials, particularly *Aquificae* and *Betaproteobacteria*, could contain hydrogen or carbon monoxide oxidizers typical of other volcanic or hydrothermal environments (Nanba *et al*., 2004; Hall *et al*., 2008). *Gammaproteobacteria*, *Firmicutes* and *Aquificae* had high relative abundance in both air and bare pyroclastic deposit samples (Fig. 3), suggesting that atmospheric deposition might contribute cells colonizing these surfaces (Smith *et al*., 2013). On the other hand, 70.0% of the individual taxa found on bare pyroclastic deposits were also found in legacy soils, in comparison with only 9.7% also found in air samples (Fig. S3), suggesting that local aeolian redistribution of pre-eruption legacy soils is more important in determining bacterial diversity on the new pyroclastic deposits (Sabacka *et al*., 2012; Walker *et al*., 2013). The island has no known springs or geothermal connections to the volcano crater that might facilitate subterranean cell dispersal (Scott *et al*., 2010). Ultimately, the activity or growth of functional taxa must be confirmed to define the prevalence of microbial autotrophy on Kasatochi Island since the 2008 eruption.

In conclusion, some combination of microbial dispersal and environmental filtering appears to be key in shaping the post-eruption trajectory of microbial community assembly, whereas the establishment of microbial community function on initially sterile pyroclastic material is closely tied to the input of OM from any source. Clearly, the re-establishment of plant, animal and microbial communities after this extreme disturbance are tightly linked in Kasatochi Island. In the Aleutian Islands region, where volcanic eruptions occur frequently on timescales of years to thousands of years, many organisms may be well adapted to recover quickly from disturbance. However, despite the evidence for flourishing microbial recovery at isolated locations on Kasatochi Island receiving OM input, microbial community structure and function five years post-eruption still differ from those of reference soils. Microbial communities are clearly sensitive to changing environmental conditions (Allison and Martiny, 2008; Shade *et al*., 2012), but sensitivity and resilience are not necessarily mutually exclusive (Shade *et al*., 2013). Biological development and ecosystem recovery in Kasatochi Island is in its early stages, and successional dynamics in microbial and macrobial structure and function may emerge over time.

Experimental procedures

Sample collection and preservation

Soil samples representative of pre- and post-eruptive surfaces with contrasting OM inputs were collected from Kasatochi Island, the location of Kasatochi Volcano (Fig. 1). Although no climatic data are available for Kasatochi Island, long-term data from nearby Adak Island (80 km west of Kasatochi) indicate a mean annual temperature of 4.7°C (monthly means, 0.4°C in February to 10.7°C in August), and mean annual precipitation of 1562 mm (monthly means, 72 mm in July to 189 mm in November) (Waythomas *et al*., 2010). Most of the soils in this region are classified as Typic Cryandepts, reflecting repeated layering of soils with modest horizon development and volcanic ash deposits (USDA, 1979; Waythomas *et al*., 2003). The eruption of Kasatochi Volcano in August 2008 deposited centimetre to metre of fine to coarse pyroclastic material over the full surface of pre-existing soils (Scott *et al*., 2010); this pyroclastic material had higher pH and much lower C content relative to pre-eruption surface soils (pH, $6.9 > 5.1$; %C, $0.08 < 1.1$; Wang *et al*., 2010). Both seabirds and vegetation re-appeared, although restricted to isolated areas, within the following year (Talbot *et al*., 2010; Williams *et al*., 2010).

As part of a 2 day biological and geological survey visit to Kasatochi Island in August 2013, sampling transects were established on bare 2008 pyroclastic deposits, and at locations where active plant growth and seabird nesting were evident. Additional transects were established on exposed pre-eruptive surface soils from former meadow and seabird rookery areas (hereafter referred to as legacy soils). From each 10 m length transect, six or seven 5 cm diameter, 10 cm depth soil core samples were collected into Whirl-Pak bags using sterile handling protocols. One transect (5 m length) included only four samples because of the small area with both bird and plant inputs on recent pyroclastic deposits. Seven cores from bird inputs on recent pyroclastic deposits only reached 2–5 cm depth because of shallowly underlying talus. Additionally, one transect of surface soil samples from Adak Island, underlying the same dominant plant species that currently dominates vegetation recovery on Kasatochi (*Leymus mollis*), was collected for reference. This resulted in the collection of 12 samples from bare pyroclastic surfaces, 13 from pyroclastic materials with post-eruptive plant growth, 6 from pyroclastic materials with bird inputs, 4 from pyroclastic materials with bird and plant inputs, 13 from pre-eruptive legacy soils with post-eruptive plant inputs, 6 from legacy soils with no plant inputs and 6 from a nearby reference site. Finally, two samples of wet + dry atmospheric deposition ('air' samples) were collected, as the accumulation of inputs to a sterilized container open to the atmosphere on the top deck of the research vessel for 12–24 h during transit between Kasatochi and Adak Islands (one sample collected in each direction). All soil samples were transported on ice to the shipboard laboratory within 6–8 h, where 2 g of subsamples were flash-frozen in a dry shipper (pre-cooled with liquid N_2) for DNA analysis and the remaining soil was frozen to −20°C. 'Air' samples were flash-frozen immediately after collection. The total soil and DNA subsamples were returned to −20°C storage within 2 weeks and −80°C storage within 1 week, respectively, at the USGS Molecular Ecology Laboratory in Anchorage, AK, where they remained until further analysis.

Soil geochemistry

Soil gravimetric water content was measured as mass lost from soil after drying at 105°C overnight. Additional soil geochemical analysis was performed at the Palmer Plant and

Soils Analysis Laboratory of the University of Alaska Fairbanks (Palmer, AK), following standard U.S. Department of Agriculture National Resources Conservation Service (USDA-NRCS) procedures (NRCS Soil Survey Staff, 1996; Wang *et al*., 2010). Soil pH was measured in 1:1 soil : deionized water. Total C and N were measured using a LECO CHN analyser, and C : N was calculated as the molar ratio of these totals. Extractable nitrate (NO_3^--N) and ammonium (NH_4^+-N) were measured colorimetrically from 2 M KCl extractant solution. Extractable phosphorus (P) was measured colorimetrically from Mehlich-3 extractant solution. Soil cations (K^+, Na^+, Ca^{2+} and Mg^{2+}) were extracted with neutral 1 M ammonium acetate and quantified using inductively coupled plasma atomic-emission spectroscopy, and BS was calculated as the total millequivalents (meq) of soil cations. In these samples, BS can be quite high due to rapid weathering of new pyroclastic materials (Wang *et al*., 2010). Cation exchange capacity (CEC) was measured using steam distillation and titration of NH_4^+-N retained within the leached soil. There was too low a volume of soil to measure EC for eight samples.

EEA assays

Soil hydrolytic and oxidative EEA potentials were measured using short-term room temperature incubations of soil in suspension with saturating concentrations of fluorometric or colorimetric organic substrates (Saiya-Cork *et al*., 2002; Zeglin *et al*., 2013). Hydrolytic assays with fluorometric substrates (AMC or MUB) were run for Phos (EC 3.1.3.1, 4-MUB-phosphate, 2 h assay), LAP (EC 3.4.11.1, L-leucine-7-amido-4-methylcoumarin, 18 h assay), CBH (EC 3.2.1.91, 4-MUB-*β-D*-cellobioside, 4 h assay), βG (EC 3.2.1.21, 4-MUB-*β-D*-glucoside, 2 h assay) and β- NAG (EC 3.2.1.14, 4-MUB-*N*-acetyl-*β-D*-glucosaminide, 4 h assay) enzyme classes, all at a final substrate concentration of 40 μM. Oxidative enzyme assays with the colorimetric L-DOPA substrate included phenol oxidase (EC 1.10.3.2, L-DOPA, 18 h assay) and peroxidase (EC 1.11.1.7, L-DOPA plus 0.12% H_2O_2, 18 h assay) enzyme classes, both run at a final substrate concentration of 5 mM. All assays were run in 96-well plates in pH 5.0 sodium acetate buffer with six to eight internal technical replicates, calculated using blank and quench controls for each soil sample, and final activities were normalized by grams of OM (estimated as soil %C/0.45/100) to enable comparison with values from other soils globally.

DNA extraction, quantitative polymerase chain reaction (qPCR) and Illumina sequencing

Total genomic DNA (gDNA) was extracted from 0.5–1.5 g of each soil sample using physical lysis, Cetyltrimethylammonium Bromide (CTAB) and phenol : chloroform extraction and overnight precipitation in PEG 6000 (DeAngelis *et al*., 2010), and gDNA yield was quantified using a Quant-iT PicoGreen assay kit (Life Technologies, Grand Island, NY) and standardized per gram of dry soil. For air samples, gDNA was extracted from 8–10 ml of accumulated atmospheric condensation using the same protocol.

qPCR assays were run on a Bio-Rad CFX CONNECT system with Bio-Rad SsoAdvanced Universal SYBR Green Supermix (Bio-Rad Laboratories, Hercules, CA, USA), using 1–10 ng template soil gDNA, 20 μL assay volume and 0.04% final BSA concentration for all assays, 100 nM final primer concentrations for the 16S rRNA gene and 500 nM final primer concentrations for fungal ITS, and primer sequences and thermal cycler programs following Fierer *et al*. (2005). Standard curves for bacterial 16S rRNA gene quantification were produced with 8.3×10^0 to 8.3×10^{-4} ng *Lactobacillus acidophilus* genomic DNA (efficiency = 95–105%, $R^2 = 0.9978$–0.9997), and for fungal ITS quantification were produced with 2.2×10^0 to 2.2×10^{-5} ng *Saccharomyces cerevisiae* genomic DNA (efficiency = 85–90%, $R^2 = 0.9989$–0.9997). All assays included no-template controls and melting curves, which confirmed that only gene copies from template soil gDNA were quantified, and three technical replicates were run per sample.

Bacterial 16S rRNA gene amplicons were prepared for Illumina sequencing and combined into one multiplexed library using bacterial universal primers (515F/806R) and Earth MicroBiome Project protocols (Caporaso *et al*., 2012), with one modification: PCR was run using 30 cycles instead of 35. Sequencing was performed using two 2×150 paired-end cycles runs on Illumina MiSeq, each including a 15% PhiX spike. Using the QIIME software package (Caporaso *et al*., 2010), raw Illumina sequence data were quality filtered, joined and demultiplexed, and assigned to OTUs (representing 97% DNA sequence similarity) that were picked using the open-reference workflow. Taxonomy was assigned using the RDP classifier, OTU sequences were aligned to the GreenGenes 16S rRNA gene reference database, and non-aligned OTUs, chimeric sequences (identified using ChimeraSlayer) and OTUs with two or fewer reads were removed from analysis. The final data set included 7 125 506 high-quality reads and 33 749 total OTUs, and the rarefied data set included 1 635 300 high-quality reads and 18 079 total OTUs. The representative sequence data have been submitted to the GenBank database under accession Nos. KP904433 – KP938182.

Statistical analysis

All data on soil geochemistry and biological properties (DNA yield, activity, taxonomic group relative abundance, diversity metrics) were checked for normality and variables were either log-transformed (soil %C, %N, extractable NO_3^-, NH_4^+ and P, 16S and ITS copy numbers, ITS:16S gene copy ratios and DNA yield) or ln-transformed (EEA activities) to meet assumptions of normality. PCA of enzyme activity data was used to reduce the seven EEA variables to an ordination of two axes of shared variation. The individual and interactive effects of the presence of legacy, plant or bird-input OM on all variables (including ordination axis scores) were evaluated using three-way analysis of variance (ANOVA). Also, the strength of correlations between ordination axis scores and geochemical and microbial variables were evaluated using Pearson's R coefficient. The significance threshold was set to $\alpha = 0.05$ for all ANOVA tests and correlation analyses. These analyses were run using R COMMANDER (Fox, 2005; R Core Development Team, 2010). Values from reference samples are shown for reference and were included in ordination and correlation tests, but were not included in ANOVA tests.

ANOVA interaction effects noted in the text do not confound interpretations made in the discussion.

For all variables derived from the 16S rRNA gene sequence data, including all diversity metrics and phyla-relative abundance, the analysed data set was reduced from 62 to 58 samples (including 56 soil samples and 2 'air' samples), based on a threshold of 28 200 reads per sample as determined by examining rarefaction curves of OTU discovery for each sample in QIIME. Archaeal sequences were present in the libraries (0.5% of total reads) and were omitted from further analysis because *Archaea* were not a focus of the study. Diversity metrics, including Chao1 estimated OTU richness, Shannon's diversity, evenness (as equitability) and Bray–Curtis dissimilarity, were calculated at this reads per sample threshold using QIIME. The matrix of Bray–Curtis dissimilarity among samples was exported from QIIME to R, then input to a NMDS ordination analysis (metaMDS, monoMDS) and a PERMANOVA among legacy, plant and bird-input sample groupings (adonis) with the vegan package. Lists of core OTUs for each sample grouping ('core' was defined as occurrence of an OTU in at least two samples from each group) were exported from QIIME and input to VENNY (Oliveros, 2007) to create Venn diagrams of OTU overlap among sample groups, and a list of core 'Bird' OTUs (occurrence of an OTU in 100% of bird-impacted samples) was also exported.

Acknowledgements

This work was undertaken with the support of the U. S. Geological Survey (USGS) Mendenhall Fellowship Program (to LHZ), the USGS Alaska Regional Director's Office and the U. S. Fish and Wildlife Service (USFWS) Alaska Maritime National Wildlife Refuge (AMNWR). Valuable field expertise was provided by Steve Talbot (USFWS Alaska Region), Jeff Williams and the captain and crew of the Research Vessel Tiglax (USFWS AMNWR), and expert lab advice was provided by Kevin Sage and Sarah Sonsthagen. Ari Jumponnen provided useful comments on the manuscript, and we also appreciate the constructive feedback of the reviewers of this manuscript. All authors declare no conflict of interest; and any use of trade, product or firm name in this publication is for descriptive purposes only and does not imply endorsement by the U. S. Government.

References

Allison, S.D. (2005) Cheaters, diffusion and nutrients constrain decomposition by microbial enzymes in spatially structured environments. *Ecol Lett* **8:** 626–635.

Allison, S.D., and Martiny, J.B.H. (2008) Resistance, resilience, and redundancy in microbial communities. *Proc Natl Acad Sci U S A* **105** (Suppl. 1): 11512–11519.

Bhattacharya, A.N., and Fontenot, J.P. (1965) Utilization of different levels of poultry litter nitrogen by sheep. *J Anim Sci* **24:** 1174–1178.

Caporaso, J.G., Kuczynski, J., Stombaugh, J., Bittinger, K., Bushman, F.D., Costello, E.K., *et al*. (2010) QIIME allows analysis of high-throughput community sequencing data. *Nat Methods* **7:** 335–336.

Caporaso, J.G., Lauber, C.L., Walters, W.A., Berg-Lyons, D., Huntley, J., Fierer, N., *et al*. (2012) Ultra-high-throughput microbial community analysis on the Illumina HiSeq and MiSeq platforms. *ISME J* **6:** 1621–1624.

Cockell, C.S., Olsson, K., Knowles, F., Kelly, L., Herrera, A., Thorsteinsson, T., and Marteinsson, V. (2009) Bacteria in weathered basaltic glass, Iceland. *Geomicrobiol J* **26:** 491–507.

Croll, D.A., Maron, J.L., Estes, J.A., Danner, E.M., and Byrd, G.V. (2005) Introduced predators transform subarctic islands from grassland to tundra. *Science* **307:** 1959–1961.

DeAngelis, K.M., Silver, W.L., Thompson, A.W., and Firestone, M.K. (2010) Microbial communities acclimate to recurring changes in soil redox potential status. *Environ Microbiol* **12:** 3137–3149.

DeGange, A.R., Byrd, G.V., Walker, L.R., and Waythomas, C.F. (2010) Introduction – The impacts of the 2008 eruption of Kasatochi Volcano on terrestrial and marine ecosystems in the Aleutian Islands, Alaska. *Arctic Antarct Alp Res* **42:** 245–249.

Fenchel, T., King, G.M., and Blackburn, H. (2000) *Bacterial Biogeochemistry: The ecophysiology of mineral cycling*. London. San Diego, CA, USA: Academic Press.

Fierer, N., Jackson, J.A., Vilgalys, R., and Jackson, R.B. (2005) Assessment of soil microbial community structure by use of taxon-specific quantitative PCR assays. *Appl Environ Microbiol* **71:** 4117–4120.

Fierer, N., Bradford, M.A., and Jackson, R.B. (2007) Toward an ecological classification of soil bacteria. *Ecology* **88:** 1354–1364.

Fierer, N., Strickland, M.S., Liptzin, D., Bradford, M.A., and Cleveland, C.C. (2009) Global patterns in belowground communities. *Ecol Lett* **12:** 1238–1249.

Fierer, N., Nemergut, D., Knight, R., and Craine, J.M. (2010) Changes through time: integrating microorganisms into the study of succession. *Res Microbiol* **161:** 635–642.

Fierer, N., Ladau, J., Clemente, J.C., Leff, J.W., Owens, S.M., Pollard, K.S., *et al*. (2013) Reconstructing the microbial diversity and function of pre-agricultural tallgrass prairie soils in the United States. *Science* **342:** 621–624.

Fox, J. (2005) The R Commander: a basic-statistics graphic user interface to R. *J Stat Softw* **19:** 1–42.

Griffiths, B.S., Ritz, K., Ebblewhite, N., and Dobson, G. (1999) Soil microbial community structure: effects of substrate loading rates. *Soil Biol Biochem* **31:** 145–153.

Hall, J.R., Mitchell, K.R., Jackson-Weaver, O., Kooser, A.S., Cron, B.R., Crossey, L.J., and Takacs-Vesbach, C.D. (2008) Molecular characterization of the diversity and distribution of a thermal spring microbial community by using rRNA and metabolic genes. *Appl Environ Microbiol* **74:** 4910–4922.

Halvorson, J.J., and Smith, J.L. (2009) Carbon and nitrogen accumulation and microbial activity in Mount St. Helens pyroclastic substrates after 25 years. *Plant Soil* **315:** 211–228.

Halvorson, J.J., Franz, E.H., Smith, J.L., and Black, R.A. (1992) Nitrogenase ativity, nitrogen-fixation and nitrogen inputs by lupines at Mount St-Helens. *Ecology* **73:** 87–98.

Halvorson, J.J., Smith, J.L., and Kennedy, A.C. (2005) Lupine effects on soil development and function during

early primary succession at Mount St. Helens. In *Ecological Responses to the 1980 Eruption of Mount St Helens*. Dale, V.H., Swanson, F.J., and Crisafulli, C.M. (eds). New York, NY, USA: Springer Science+Business Media, pp. 243–254.

Ibekwe, A.M., Kennedy, A.C., Halvorson, J.J., and Yang, C.H. (2007) Characterization of developing microbial communities in Mount St. Helens pyroclastic substrate. *Soil Biol Biochem* **39:** 2496–2507.

Jicha, B.R., Scholl, D.W., Singer, B.S., Yogodzinski, G.M., and Kay, S.M. (2006) Revised age of Aleutian Island Arc formation implies high rate of magma production. *Geology* **34:** 661–664.

Kim, S.B., and Nedashkovskaya, O.I. (2012) *Genus XXIV.* Salinibacterium. In *Bergey's Manual of Systematic Bacteriology, Second Edition, Volume 5, The Actinobacteria, Part A and B*. Goodfellow, M., Kampfer, P., Busse, H.-J., Trujilo, M.E., Suzuki, K.-I., Ludwig, W., and Whitman, W.B. (eds). New York, NY, USA: Springer, pp. 969–972.

King, G.M. (2003) Contributions of atmospheric CO and hydrogen uptake to microbial dynamics on recent Hawaiian volcanic deposits. *Appl Environ Microbiol* **69:** 4067–4075.

Klappenbach, J.A., Dunbar, J.M., and Schmidt, T.M. (2000) rRNA operon copy number reflects ecological strategies of bacteria. *Appl Environ Microbiol* **66:** 1328–1333.

Lauber, C.L., Hamady, M., Knight, R., and Fierer, N. (2009) Pyrosequencing-based assessment of soil pH as a predictor of soil bacterial community structure at the continental scale. *Appl Environ Microbiol* **75:** 5111–5120.

Leblans, N.I.W., Sigurdsson, B.D., Roefs, P., Thuys, R., Magnusson, B., and Janssens, I.A. (2014) Effects of seabird nitrogen input on biomass and carbon accumulation after 50 years of primary succession on a young volcanic island, Surtsey. *Biogeosci* **11:** 6237–6250.

Logue, J.B., Mouquet, N., Peter, H., Hillebrand, H., and Metacommunity Working, G. (2011) Empirical approaches to metacommunities: a review and comparison with theory. *Trends Ecol Evol* **26:** 482–491.

Michaelson, G.J., Wang, B., and Ping, C.L. (2015) Kasatochi Island volcano: fertility of the early post-eruptive surfaces. *Arctic Antarct Alp Res*. in review.

Miller, T.P., McGimsey, R.G., Richter, D.H., Riehle, J.R., Nye, C.J., Yount, M.E., and Dumoulin, J.A. (1998) Catalog of the historically active volcanoes of Alaska. US Geological Survey Open-File Report.

Nanba, K., King, G.M., and Dunfield, K. (2004) Analysis of facultative lithotroph distribution and diversity on volcanic deposits by use of the large subunit of ribulose 1,5-bisphosphate carboxylase/oxygenase. *Appl Environ Microbiol* **70:** 2245–2253.

Nemergut, D.R., Anderson, S.P., Cleveland, C.C., Martin, A.P., Miller, A.E., Seimon, A., and Schmidt, S.K. (2007) Microbial community succession in an unvegetated, recently deglaciated soil. *Microb Ecol* **53:** 110–122.

Odum, E.P. (1969) The strategy of ecosystem development. *Science* **164:** 262–270.

Oliveros, J.C. (2007). *VENNY. An interactive tool for comparing lists with Venn Diagrams* [WWW document]. URL http://bioinfogp.cnb.csic.es/tools/venny/index.html.

Philippot, L., Andersson, S.G.E., Battin, T.J., Prosser, J.I., Schimel, J.P., Whitman, W.B., and Hallin, S. (2010) The ecological coherence of high bacterial taxonomic ranks. *Nat Rev Micro* **8:** 523–529.

R Core Development Team (2010) *R: A Language and Environment for Statistical Computing*. R Foundation for Statistical Computing, Vienna, Austria. ISBN 3-900051-07-0, URL http://www.R-project.org/.

Rousk, J., Baath, E., Brookes, P.C., Lauber, C.L., Lozupone, C., Caporaso, J.G., *et al*. (2010) Soil bacterial and fungal communities across a pH gradient in an arable soil. *ISME J* **4:** 1340–1351.

Sabacka, M., Priscu, J.C., Basagic, H.J., Fountain, A.G., Wall, D.H., Virginia, R.A., and Greenwood, M.C. (2012) Aeolian flux of biotic and abiotic material in Taylor Valley, Antarctica. *Geomorphology* **155:** 102–111.

Saiya-Cork, K.R., Sinsabaugh, R.L., and Zak, D.R. (2002) The effects of long term nitrogen deposition on extracellular enzyme activity in an *Acer saccharum* forest soil. *Soil Biol Biochem* **34:** 1309–1315.

Schlesinger, W.H. (1997) *Biogeochemistry: An Analysis of Global Change*. San Diego, CA, USA: Harcourt Press.

Scott, W.E., Nye, C.J., Waythomas, C.F., and Neal, C.A. (2010) August 2008 eruption of Kasatochi Volcano, Aleutian Islands, Alaska – Resetting an island landscape. *Arctic Antarct Alp Res* **42:** 250–259.

Shade, A., Peter, H., Allison, S.D., Baho, D.L., Berga, M., Burgmann, H., *et al*. (2012) Fundamentals of microbial community resistance and resilience. *Front Microbiol* **3:** 417.

Shade, A., Caporaso, J.G., Handelsman, J., Knight, R., and Fierer, N. (2013) A meta-analysis of changes in bacterial and archaeal communities with time. *ISME J* **7:** 1493–1506.

Sinsabaugh, R.L., Lauber, C.L., Weintraub, M.N., Ahmed, B., Allison, S.D., Crenshaw, C., *et al*. (2008) Stoichiometry of soil enzyme activity at global scale. *Ecol Lett* **11:** 1252–1264.

Smith, D.J., Timonen, H.J., Jaffe, D.A., Griffin, D.W., Birmele, M.N., Perry, K.D., *et al*. (2013) Intercontinental dispersal of bacteria and archaea by transpacific winds. *Appl Environ Microbiol* **79:** 1134–1139.

Talbot, S.S., Talbot, S.L., and Walker, L.R. (2010) Post-eruption legacy effects and their implications for long-term recovery of the vegetation on Kasatochi Island, Alaska. *Arctic Antarct Alp Res* **42:** 285–296.

USDA NRCS Soil Survey Staff (1996) Soil survey laboratory methods manual. Washington, D.C., USA.

USDA, Soil Conservation Service (1979) Exploratory soil survey of Alaska.

Vitousek, P.M., and Farrington, H. (1997) Nutrient limitation and soil development: experimental test of a biogeochemical theory. *Biogeochemistry* **37:** 63–75.

Walker, L.R., Sikes, D.S., DeGange, A.R., Jewett, S.C., Michaelson, G., Talbot, S.L., *et al*. (2013) Biological legacies direct early ecosystem recovery and food web reorganization after a volcanic eruption in Alaska. *Ecoscience* **20:** 240–251.

Wang, B., Michaelson, G., Ping, C.L., Plumlee, G., and Hageman, P. (2010) Characterization of pyroclastic deposits and pre-eruptive soils following the 2008 eruption of Kasatochi Island Volcano, Alaska. *Arctic Antarct Alp Res* **42:** 276–284.

Waythomas, C.F., Miller, T.P., and Nye, C.J. (2003) Geology and late Quaternary eruptive history of Kanaga Volcano, a calc-alkaline stratovolcano in the western Aleutian Islands, Alaska. In *Studies by the US Geological Survey in Alaska, 2001*. Galloway, J.P. (ed.). U.S. Geological Survey Professional Paper 1678, pp. 181–197.

Waythomas, C.F., Scott, W.E., and Nye, C.J. (2010) The geomorphology of an Aleutian Volcano following a major eruption: the 7–8 August 2008 eruption of Kasatochi Volcano, Alaska, and its aftermath. *Arctic Antarct Alp Res* **42:** 260–275.

Whitman, W.B., Coleman, D.C., and Wiebe, W.J. (1998) Prokaryotes: the unseen majority. *Proc Natl Acad Sci USA* **95:** 6578–6583.

Williams, J.C., Drummond, B.A., and Buxton, R.T. (2010) Initial effects of the August 2008 volcanic eruption on breeding birds and marine mammals at Kasatochi Island, Alaska. *Arctic Antarct Alp Res* **42:** 306–314.

Wu, L.L., Jacobson, A.D., Chen, H.C., and Hausner, M. (2007) Characterization of elemental release during microbe-basalt interactions at T = 28 degrees C. *Geochim Cosmochim Acta* **71:** 2224–2239.

Yarwood, S.A., Bottomley, P.J., and Myrold, D.D. (2010) Soil microbial communities associated with Douglas-fir and Red Alder stands at high- and low-productivity forest sites in Oregon, USA. *Microb Ecol* **60:** 606–617.

Zeglin, L.H., Sinsabaugh, R.L., Barrett, J.E., Gooseff, M.N., and Takacs-Vesbach, C.D. (2009) Landscape distribution of microbial activity in the McMurdo Dry Valleys: linked biotic processes, hydrology, and geochemistry in a cold desert ecosystem. *Ecosyst* **12:** 562–573.

Zeglin, L.H., Bottomley, P.J., Jumpponen, A., Rice, C.W., Arango, M., Lindsley, A., *et al*. (2013) Altered precipitation regime affects the function and composition of soil microbial communities on multiple time scales. *Ecology* **94:** 2334–2345.

Zehetner, F. (2010) Does organic carbon sequestration in volcanic soils offset volcanic CO_2 emissions? *Quaternary Sci Rev* **29:** 1313–1316.

Supporting information

Additional Supporting Information may be found in the online version of this article at the publisher's web-site:

Fig. S1. Scatterplots of soil % carbon versus soil extracellular enzyme activity potentials (A–F) per g dry soil and (G–L) per g OM; versus soil fungal ITS copy number (M) per g dry soil and (N) per g OM; and versus (O) fungal ITS: bacterial 16S rRNA gene copy ratio, with different symbols for contrasting OM input categories including highlighted differentiation of legacy soils from the buried bird colony.

Fig. S2. Principal components analysis (PCA) ordination of extracellular enzyme activity potential (A) and non-metric multidimensional scaling ordination (NMDS) of the relative abundance of 97% similar bacterial 16S rRNA gene taxonomic units (B) for each OM input category, with all replicate samples shown, and vectors of significant ($P \leq 0.05$) correlation with geochemical and other microbial factors overlaid. Mean values are shown in Fig. 2 and Fig. 3, and individual enzyme activity loadings and correlations of axes with major taxonomic group abundances are shown in Table 1.

Fig. S3. Venn diagrams showing overlap of core 97% similar OTUs (OTUs found in at least 2 samples per category, expressed as a percent of total OTUs) among (A) bare pyroclastic materials, pre-eruptive legacy soils, air samples and reference soils and among (B) bare pyroclastic materials and pyroclastics with plant, bird and both plant and bird OM inputs.

Table S1. Soil geochemical characteristics in organic matter input categories, arithmetic mean (1SE).

Table S2. Soil extracellular enzyme activities (EEA) in organic matter input categories, arithmetic mean (1SE).

Table S3. Correlations of extracellular enzyme activity PCA axis and bacterial 16S rRNA gene NMDS axes with soil chemical and microbial properties.

Table S4. Soil microbial biomass, domain level population size and diversity in organic matter input categories, arithmetic mean (1SE).

Table S5. Soil bacterial phyla and subphyla percent relative population size in organic matter input categories, arithmetic mean (1SE).

Text S1. List of core OTUs found in all samples with bird OM inputs (both legacy soil and new pyroclastics).